IEEE Access
Multidisciplinary | Rapid Review | Open Access Journal

IEEE POWER & ENERGY SOCIETY SECTION

Received January 31, 2020, accepted February 29, 2020, date of publication March 9, 2020, date of current version March 17, 2020.

Digital Object Identifier 10.1109/ACCESS.2020.2979317

Probabilistic Load Flow Based on Bivariate Dimension Reduction and Johnson System

HANG LI, ZHE ZHANG, AND XIANGGEN YIN, (Member, IEEE)
State Key Laboratory of Advanced Electromagnetic Engineering and Technology, Huazhong University of Science and Technology, Wuhan 430074, China
Corresponding author: Hang Li (leehang@outlook.com)

This work was supported in part by the National High Technology Research and Development Program of China (863 Program) under Grant 2015AA050201.

ABSTRACT A probabilistic load flow (PLF) is an effective tool that helps describe the uncertainty of power system operation. However, when confronting random variables with non-Gaussian distributions and highly discrete characteristics, existing PLF methods have difficulty balancing efficiency and accuracy. Therefore, a novel approach based on bivariate dimension reduction (BDR) and the Johnson system is proposed herein. BDR is used to estimate the moments of output random variables (ORVs). Because BDR considers the joint effect of input random variables, it significantly reduces the estimation error for high-order moments in particular. In addition, a strategy to improve BDR efficiency is proposed. The Johnson system is used to obtain the probability distributions of ORVs as it has better adaptability and accuracy than the series expansion method. Case studies including comparisons between this approach and others found in the literature were conducted, and the results obtained showed that the proposed method has better performance than previous approaches.

INDEX TERMS Bivariate dimension reduction, Johnson system, probabilistic load flow, renewable energy source.

I. INTRODUCTION

The number of renewable energy sources (RESs), such as wind and photovoltaic power, that are being consumed is increasing annually. While RESs provide tremendous economic benefits, they considerably increase the operational uncertainty of power systems, rendering safe and stable operation difficult.

In highly uncertain situations, traditional deterministic methods are often less useful than probabilistic ones. The concept of probabilistic load flow (PLF) [1] has therefore recently attracted considerable attention as a valuable tool for describing the operating status of power systems.

Since the concept emerged, various PLF methods have been developed. These can be categorized as simulation, analytical, and approximation methods [2]. The accuracy and efficiency of the calculated results are two important indices considered in evaluating the performance of individual methods.

Simulation methods include the Monte Carlo simulation method (MCSM) and various improved methods [3]–[6] based on it. Through several sampling and deterministic load flow (DLF) computations, accuracy is guaranteed. Unfortunately, such methods are quite time consuming, and are therefore mainly employed as reference standards to evaluate the accuracy of other methods.

Cumulant method (CM) [7]–[16] is the representative of the analytical method. It can easily and efficiently calculate the cumulants of the output random variables (ORVs) based on the linearized load flow model and the characteristics of the cumulant. Although CM performs well in terms of efficiency, its accuracy is less impressive: a considerable error is observed when the input random variables (IRVs) are highly discrete [16].

Point estimate method (PEM) [17]–[25] is the representative of the approximation method. Computationally, PEM is also efficient. It constructs orthogonal polynomials to approximate the implicit function relating IRVs to ORVs; thus, the moments of the ORVs can be estimated. Hong's $2m + 1$ PEM scheme [18], [19] appears to be the most commonly applied scheme; it only requires $2m + 1$ times DLFs when m IRVs are considered; however, it exhibits poor performance for estimating high-order moments. Singular value decomposition [20] and Nataf transformation [21] is combined with PEM, which makes this method available for large-scale power systems and correlated IRVs. In recent years,

The associate editor coordinating the review of this manuscript and approving it for publication was Pierluigi Siano.

univariate dimension reduction (UDR) [22]–[25] is proposed as an improved PEM, which has better accuracy than Hong's scheme. Although many improvements to PEM have been proposed, it still faces difficulties in accurately estimating the high-order moments of ORVs, such as skewness and kurtosis, which are important parameters in describing the distribution shape of a non-Gaussian variable.

Sparse polynomial chaos expansion (sPce) [26], [27] is another candidate. It uses a surrogate model instead of nonlinear AC load flow equations to solve the PLF problem, which can balance efficiency and accuracy. However, making the proper choice of numbers of DLF in advance to obtain a reasonable surrogate is difficult, and no analytical expression of PDF and CDF is available that may cause inconvenience in the application of this method.

As cumulant and moment can be easily transformed into each other [7], CM and PEM can also be classified into the moment-based PLF method. Evidently, only knowing moments of ORVs is typically insufficient in practical use. Therefore, the series expansion method (SEM), such as the Gram–Charlier series [7], [11] and Cornish–Fisher series [8], [12] is commonly utilized to approximate probability distributions according to moments. Despite its popularity, SEM has major defects: 1) The ORVs' skewness and kurtosis are limited, or SEM will generate illegitimate negative probability distribution functions [28]; 2) the approximation accuracy is not directly proportional to the number of terms [7], therefore, it is hard to determine the proper terms used in advance; 3) large errors are commonly observed in the tail area. However, for some applications based on PLF, such as chance-constrained optimization [29], the tail area is of interest. Maximum entropy [15] is another method that attempts to improve PDF approximation accuracy. However, this method requires the correct range of the ORV, which is difficult to obtain for the moment-based method.

In practice, the uncertainties of RES outputs are highly discrete (a problem for CM) and usually follow a non-Gaussian distribution with correlation (a problem for PEM), whereas applications based on PLF increasingly require high efficiency (a problem for MCSM). Therefore, new schemes for PLF that are both accurate and efficient would be of great interest. This paper proposes a new PLF method based on the bivariate dimension reduction (BDR) and the Johnson system [30], [31]. The contributions of this study are as follows.

1) BDR is an improvement over UDR. To the best of the authors' knowledge, this is the first time that BDR has been used to solve the PLF problem, through which the first four moments of ORVs have been accurately estimated. Moreover, a strategy is proposed to improve BDR efficiency.

2) The Johnson system is used to approximate the PDF or CDF of ORVs as it is more accurate than SEM and works well with BDR. Furthermore, the analytical expression of PDF or CDF can be obtained through the Johnson system, which will benefit the applications based on PLF.

The remainder of this paper is organized as follows. The theoretical background related to PLF calculation and the Nataf transformation is introduced in Section II. Section III describes the proposed method. In Section IV, the procedure of the proposed PLF method is presented, and in Section V, case studies are performed. Finally, the conclusions drawn are presented in Section VI.

II. PROBLEM BACKGROUND

A. PROBLEM FORMULATION

The load flow equations describe the relationship between IRVs and ORVs. A concise manner of representing this relationship is

$$\mathbf{Y} = G(\mathbf{X}) \tag{1}$$

where $\mathbf{X} = [x_1, x_2, \cdots x_n]^{\mathrm{T}}$ is the vector of IRVs; $\mathbf{Y} = [y_1, y_2, \cdots y_m]^{\mathrm{T}}$ is the vector of ORVs; and $G(\cdot)$ represents the functional dependence in the load flow equations in the AC formulation.

The IRVs influence the result of a load flow calculation. While there is no limit to the number or type of IRVs, in practice, some variables are either predictable or have an insignificant influence. In this study, active and reactive bus power injections are considered to be IRVs with arbitrary distributions. The ORVs include bus voltage magnitudes V and angles θ as well as branch active flows P and reactive flows Q, whose distributions are determined by the IRVs' distribution and load flow equations.

The central moments of $\mathbf{Y}$ are given by:

$$\mathrm{E}(\mathbf{Y}^l) = E[G^l(\mathbf{X})] = \int G^l(\mathbf{X})\, f_{\mathbf{X}}(\mathbf{X})\mathrm{d}\mathbf{x} \tag{2}$$

where $\mathrm{E}(\cdot)$ is the expectation operator, l denotes the l^{th} central moment, and $f_{\mathbf{X}}(\mathbf{X})$ represents the joint probability density function (PDF) of $\mathbf{X}$.

According to (2), each moment is calculated through n-dimensional integration. However, such integration is difficult for the following reasons: 1) $f_{\mathbf{X}}(\mathbf{X})$ is often complicated and may even be impossible to express analytically; 2) high-dimensional integration in general is difficult and time-consuming.

Our proposed method identifies the proper transformation and dimensionality reduction to reduce the computational difficulty and effort without compromising accuracy. We then use the obtained moments and the Johnson system to approximate the probability distributions of the ORVs.

B. NATAF TRANSFORMATION

The Nataf transformation [21], [32] is an effective tool that can project an independent standard Gaussian space to the original integral space represented in (2). Thus, the correlation issue is well handled and the joint PDF $f_{\mathbf{X}}(\mathbf{X})$ is replaced by the product of the PDFs of independent standard Gaussian variables; this will benefit the subsequent implementation of the proposed method.

According to the Nataf transformation [21], the IRV vector $\mathbf{X}$ is transformed from the independent standard Gaussian

random-variable vector $\mathbf{U}$ to:

$$\begin{pmatrix} u_1 \\ u_2 \\ \vdots \\ u_n \end{pmatrix} \xrightarrow{\mathbf{Z}=\mathbf{L_Z}\mathbf{U}} \begin{pmatrix} z_1 \\ z_2 \\ \vdots \\ z_n \end{pmatrix} \xrightarrow{F_i^{-1}(\Phi(z_i))} \begin{pmatrix} x_1 \\ x_2 \\ \vdots \\ x_n \end{pmatrix} = \mathbf{X} \quad (3)$$

where $\mathbf{Z}$ is the Gaussian random variable vector with correlation, $\mathbf{L_Z}$ is the lower triangular matrix from the Cholesky decomposition of the correlation coefficient matrix $\boldsymbol{\rho}_\mathbf{Z}$, $\Phi(\cdot)$ denotes the CDF of a standard Gaussian variable, and $F_i^{-1}(x_I)$, $i = 1, \cdots, n$ denotes the inverse CDF of x_i.

Assuming the correlation coefficient matrix $\boldsymbol{\rho}_\mathbf{X}$ of $\mathbf{X}$ is available, $\boldsymbol{\rho}_\mathbf{Z}$ could be obtained through the relationship between $\boldsymbol{\rho}_\mathbf{X}$ and $\boldsymbol{\rho}_\mathbf{Z}$ [32]:

$$\begin{aligned} \rho_{z_{ij}} &= \int_{-\infty}^{\infty}\int_{-\infty}^{\infty}\left(\frac{x_i-\mu_i}{\sigma_i}\right)\left(\frac{x_j-\mu_j}{\sigma_j}\right) f_{x_ix_j}(x_i,x_j)dx_idx_j \\ &= \int_{-\infty}^{\infty}\int_{-\infty}^{\infty}\left(\frac{F_i^{-1}(\Phi(z_i))-\mu_i}{\sigma_i}\right)\left(\frac{F_j^{-1}(\Phi(z_j))-\mu_j}{\sigma_j}\right) \\ &\quad \cdot\phi_{z_iz_j}(z_i,z_j,\rho_{z_{ij}})dz_idz_j \end{aligned} \quad (4)$$

where $\rho_{x_{ij}}$ and $\rho_{z_{ij}}$ are the elements in $\boldsymbol{\rho}_\boldsymbol{X}$ and $\boldsymbol{\rho}_\boldsymbol{Z}$ representing the correlation coefficient between the i^{th} and j^{th} variables in$\mathbf{X}$ and $\mathbf{Z}$; μ_i and μ_j are the expectations of IRV x_i and x_j, respectively; σ_i and σ_j are the variances of IRV x_i and x_j, respectively; and $\phi_{z_iz_j}(z_i, z_j, \rho_{zij})$ is the joint PDF of the two-dimensional standard Gaussian variables z_i and z_j with the correlation coefficient $\rho_{z_{ij}}$. In this study, $\boldsymbol{\rho}_\mathbf{Z}$ is obtained accurately and rapidly through Gauss–Hermite integration, as detailed in [32].

Combining (1) and (3), $\mathbf{Y}$ is expressed as:

$$\mathbf{Y} = G(\mathbf{X}) = G(\Phi^{-1}(F(\mathbf{X}))) = H(\mathbf{U}) \quad (5)$$

The central moments of $\mathbf{Y}$ can be calculated from the following equation instead of (2):

$$\mathrm{E}(\boldsymbol{Y}^l) = \int\cdots\int H^l(u_1,\cdots,u_n)\phi(u_1)\cdots\phi(u_n)du_1\cdots du_n \quad (6)$$

where $\phi(u_\mathrm{i})$ is the PDF of the independent standard Gaussian variable u_i. Note that the $f_\mathbf{X}(\mathbf{X})$ in (2) has been replaced in (6) by the product of the PDFs of independent standard Gaussian variables.

III. THE PROPOSED METHOD FOR PROBABILISTIC LOAD FLOW

In this section, the procedure of the proposed method that combines BDR and Johnson system are analyzed in detail.

A. THE PRINCIPLE OF BIVARIATE DIMENSION REDUCTION

Following Nataf transformation, (6) is still not easy to solve owing to the n-dimensional integrand $H(\mathbf{U})$. An effective approach to deal with this problem is to employ general dimension reduction (GDR) [33]–[35] for the integration.

The core idea of GDR is to approximate $H(\mathbf{U})$ by summing several low-dimension functions such that that the n-dimensional integration in (6) is solved by summing several low-dimensional integrations. The computation of several low-dimensional integrations is frequently much faster and easier than that of one high-dimensional integration.

According to the principle of GDR, the n-dimensional integrand $H(\mathbf{U})$ is exactly expressed as follows [35]:

$$\begin{aligned} \mathbf{Y} = H(\mathbf{U}) &= H_0 + \sum_i H_i(u_i) + \sum_{i_1<i_2} H_{i_1i_2}(u_{i_1},u_{i_2}) + \cdots \\ &\quad + \sum_{i_1<i_2<\cdots i_l} H_{i_1i_2\cdots i_l}(u_{i_1},u_{i_2},\cdots u_{i_l}) + \cdots \\ &\quad + \sum_{i_1<i_2<\cdots i_n} H_{i_1i_2\cdots i_n}(u_{i_1},u_{i_2},\cdots u_{i_n}) \end{aligned} \quad (7)$$

The various terms in (7) are expressed as follows:

$$\begin{aligned} H_0 &= H(\mathbf{U_c}) \\ H_i(u_i) &= H(u_i, \underline{\mathbf{U}}_{i,\mathbf{c}}) - H_0 \\ H_{i_1i_2}(u_{i_1},u_{i_2}) &= H(u_{i_1},u_{i_2},\underline{\mathbf{U}}_{i_1i_2,\mathbf{c}}) - H_{i_1}(u_{i_1}) - H_{i_2}(u_{i_2}) - H_0 \\ &\quad \vdots \\ H_{i_1\cdots i_l}(u_{i_1},\cdots,u_{i_l}) &= H_{i_1i_2\cdots i_l}(u_{i_1},u_{i_2},\cdots u_{i_l},\underline{\mathbf{U}}_{i_1i_2\cdots i_l,\mathbf{c}}) \\ &\quad - \sum_{\{j_1j_2\cdots j_{l-1}\}\subset\{i_1i_2\cdots i_l\}} H_{j_1j_2\cdots j_{l-1}}(u_{j_1},u_{j_2},\cdots u_{j_{l-1}}) \\ &\quad - \sum_{\{j_1j_2\cdots j_{l-2}\}\subset\{i_1i_2\cdots i_l\}} H_{j_1j_2\cdots j_{l-2}}(u_{j_1},u_{j_2},\cdots u_{j_{l-2}}) - \cdots \\ &\quad - \sum_{j\subset\{i_1i_2\cdots i_l\}} H_j(u_j) - H_0 \end{aligned} \quad (8)$$

Here, $\mathbf{U}_\boldsymbol{C}$ is the reference vector, which is $[0, \cdots, 0]$ in the independent standard Gaussian space; $\underline{\mathbf{U}}_{i_1i_2\cdots i_l,\boldsymbol{C}}$ is formulated after eliminating the sub-vectors of $\mathbf{U}_\boldsymbol{C}$ corresponding to $u_{i_1}, u_{i_2}, \cdots, u_{i_l}$, $H_i(u_i)$ represents the effects of the variable u_i on $\mathbf{Y}$; $H_{i_1,i_2\cdots i_l}(u_{i_1}, u_{i_2}, \cdots, u_{i_l})$ represents the joint effects of all variables $u_{i_1}, u_{i_2}, \cdots, u_{i_l}$ on $\mathbf{Y}$.

By truncating (7), $H(\mathbf{U})$ is approximated by the following equation:

$$\begin{aligned} H(\mathbf{U}) &\approx H_0 + \sum_i H_i(u_i) + \cdots \\ &\quad + \sum_{i_1<i_2<\cdots i_s} H_{i_1i_2\cdots i_s}(u_{i_1},u_{i_2},\cdots u_{i_s}) \end{aligned} \quad (9)$$

where s is the highest reduction dimension. Based on the value of s in (9), the approximation of $H(\mathbf{U})$ can be classified into the univariate dimension reduction (UDR), where $s = 1$, and the multivariate dimension reduction (MDR), where $s > 1$ and $s \ll n$.

UDR has been proven to be equivalent to Zhao's PEM [21]. Based on the UDR, only two terms exist on the right side of (9): one is the constant function and the other is the sum of

univariate effects functions. The multivariate functions, representing joint effects, are neglected, causing a substantially large residue error. Although the estimation accuracy for lower moments, such as expectation and variance, is acceptable, the UDR will cause large errors for high-order moments, particularly for a power system with arbitrarily large IRVs' variation and/or high nonlinearity [33].

In contrast, MDR can approximate the $H(\mathbf{U})$ to any level of precision. Even though more computation effort is involved with the MDR than with the UDR, an appropriate value of s and the efficiency enhancement strategy proposed herein will permit an acceptable balance of efficiency and precision.

B. COMPUTING MOMENTS OF OUTPUT RANDOM VARIABLES

The computation cost of MDR increases with increasing reduction dimension s. Previous works [33], [35] indicate that $s = 2$ provides a reasonable balance between the concerns of accuracy and efficiency and will always be assumed hereafter; the term BDR will refer to the $s = 2$ MDR method in the remainder of this paper.

Deploying the BDR, the integrand $H(\mathbf{U})$ is approximated as follows:

$$H(\mathbf{U}) \approx \sum_{i_1<i_2} H(u_{i_1}, u_{i_2}, \mathbf{U}_{ij,c}) - (n-2)\sum_{k=1}^{n} H(u_k, \mathbf{U}_{k,c}) + \frac{(n-1)(n-2)}{2} H_0 \quad (10)$$

Evidently, $H(\mathbf{U})$ is approximated by $n(n-1)/2$ bivariate functions, n univariate functions, and a constant function.

Combining (6) and (10), the central moments of $\mathbf{Y}$ can be expressed as follows:

$$\begin{aligned} \mathrm{E}(\mathbf{Y}^l) &\approx E[\sum_{i_1<i_2} H^l(u_{i_1}, u_{i_2}, \underline{\mathbf{U}}_{i_1 i_2,c}) - (n-2)\sum_{k=1}^{n} H^l(u_k, \underline{\mathbf{U}}_{k,c}) + \frac{(n-1)(n-2)}{2} H_0^l] \\ &= \sum_{i_1<i_2} E[H^l(u_{-i_1}, u_{i_2}, \underline{\mathbf{U}}_{i_1 i_2,c})] - (n-2)\sum_{k=1}^{n} E[H^l(u_k, \underline{\mathbf{U}}_{k,c})] + \frac{(n-1)(n-2)}{2} H_0^l \end{aligned} \quad (11)$$

where

$$\begin{aligned} E[H^l(u_k, \underline{\mathbf{U}}_{k,c})] &= \int_{-\infty}^{+\infty} H^l(u_k, \underline{\mathbf{U}}_{k,c})\phi(u_k)du_k \\ E[H^l(u_{i_1}, u_{i_2}, \underline{\mathbf{U}}_{i_1 i_2,c})] &= \int_{-\infty}^{+\infty}\int_{-\infty}^{+\infty} H^l(u_{i_1}, u_{i_2}, \underline{\mathbf{U}}_{i_1 i_2,c}) \cdot \phi(u_{i_1})\phi(u_{i_2})du_{i_1}du_{i_2} \end{aligned} \quad (12)$$

Thus, the n-dimensional integration in (6) has been transformed into the much easier summation of several one- and two-dimensional integrations in (12).

TABLE 1. Typical weights and abscissas for Gauss–Hermite quadrature.

Numbers	Abscissas	Weights
3	0	1.1816
	±1.2247	2.9541e−1
5	0	9.4530e−1
	±0.9585	3.9362e−1
	±2.0201	1.9953e−2
7	0	8.1027e−1
	±0.8162	4.2561e−1
	±1.6735	5.4512e−2
	±2.6519	9.7178e−4

Gauss–Hermite quadrature can be used to solve (12) as follows:

$$\begin{aligned} E[H^l(u_k, \underline{\mathbf{U}}_{k,c})] &= \sum_{m=1}^{r} \frac{w_{GH,m}}{\sqrt{\pi}} H^l(\sqrt{2}\alpha_{GH,m}, \underline{\mathbf{U}}_{k,c}) \\ E[H^l(u_{i_1}, u_{i_2}, \underline{\mathbf{U}}_{i_1 i_2,c})] &= \sum_{m_1=1}^{r}\sum_{m_2=1}^{r} \frac{w_{GH,m_1} w_{GH,m_2}}{\sqrt{\pi}} H^l(\sqrt{2}\alpha_{GH,m_1}, \sqrt{2}\alpha_{GH,m_2}, \underline{\mathbf{U}}_{i_1 i_2,c}) \end{aligned} \quad (13)$$

where $\alpha_{GH,m}$ and $w_{GH,m}$ are the abscissas and corresponding weights, respectively; r is the number of abscissas, usually selected to be odd. The higher the number of points, the higher the integration accuracy; however, accordingly higher is the computational burden. Table 1 lists the commonly used abscissas and their weights.

C. COMPUTATION EFFICIENCY ENHANCEMENT

The computational burden of BDR strongly depends on the number of two-dimensional integrations. In this section, we propose a strategy to reduce it.

The most time-consuming part of solving (11) is calculating the expectation of the bivariate function. According to (8), this bivariate function is given as follows:

$$H(u_{i_1}, u_{i_2}, \underline{\mathbf{U}}_{i_1 i_2,c}) = H_{i_1 i_2}(u_{i_1}, u_{i_2}) + H(u_{i_1}, \underline{\mathbf{U}}_{i_1,c}) + H(u_{i_2}, \underline{\mathbf{U}}_{i_2,c}) - H_0 \quad (14)$$

Assuming that the joint effect $H_{i_1 i_2}(u_{i_1}, u_{i_2})$ on $\mathbf{Y}$ is minor, this function can be approximated as:

$$H(u_{i_1}, u_{i_2}, \underline{\mathbf{U}}_{i_1 i_2,c}) \approx H(u_{i_1}, \underline{\mathbf{U}}_{i_1,c}) + H(u_{i_2}, \underline{\mathbf{U}}_{i_2,c}) - H_0 \quad (15)$$

which only includes a constant function and univariate functions. Therefore, by solving the constant and univariate equations first, and using the result to represent the bivariate function, the amount of calculation can be tremendously reduced.

Now, the problem is to judge whether the joint effects are indeed minor. We achieve this with one DLF by comparing the differences between (14) and (15).

First, two abscissas are selected from Table 1. Then, one DLF using the selected abscissas is performed to obtain the results of the bivariate function. The joint effect is then calculated by:

$$\begin{aligned} H_{i_1 i_2}(u_{i_1}, u_{i_2}) = {} & H(\sqrt{2}\alpha_{GH,m_1}, \sqrt{2}\alpha_{GH,m_2}, \underline{\mathbf{U}}_{i_1 i_2,c}) \\ & - H(\sqrt{2}\alpha_{GH,m_1}, \underline{\mathbf{U}}_{i_1,c}) \\ & - H(\sqrt{2}\alpha_{GH,m_2}, \underline{\mathbf{U}}_{i_2,c}) + H_0 \end{aligned} \quad (16)$$

Note that there are m variables in Y, and the joint effect $H_{i_1 i_2}(u_{i_1}, u_{i_2})$ is different for different variables in Y. Let ε represent the effect threshold: i.e., if any joint effect on the variables in Y is larger than ε, the whole joint effect should not be neglected. According to practical experience, most joint effects are far less than 0.01 and have minor influence on moment estimation results; therefore, a predetermined $\varepsilon = 0.01$ is used in this study.

D. JOHNSON SYSTEM

For practical engineering applications, only knowing the moments of the ORVs is not always sufficient: their PDF or CDF may also be of interest. In this section, the Johnson system is adopted to approximate the PDF or CDF of ORVs.

The Johnson system uses the following function to transform the ORV y (which follows an arbitrary probability distribution) into the standard Gaussian variable u [30]:

$$u = a + b \times f(\frac{y - c}{d}) \tag{17}$$

where a and b are the shape parameters, c is the position parameter, and d is the scale parameter. Regarding $(y-c)/d$ as a variable v, the function $f(v)$ has one of the following forms:

$$\begin{aligned} S_L &: f(v) = \ln(v) \\ S_U &: f(v) = \ln(v + \sqrt{v^2 + 1}) \\ S_B &: f(v) = \ln(v/(1 - v)) \\ S_N &: f(v) = v \end{aligned} \tag{18}$$

where S_L is the family of Lognormal distributions, S_U is the family of unbounded distributions (and the range of v is unlimited), S_B is the family of bounded distributions, and S_N is the family of Gaussian distributions. S_N is utilized for transformations between Gaussian distributions.

Taking the inverse transformation of (20), the distribution of y can be approximated by the standard Gaussian distribution as follows:

$$y = c + d \times f^{-1}(\frac{u - a}{b}) \tag{19}$$

Note that y is the function of the standard Gaussian variable; therefore, there is an analytical expression of y, and this feature will benefit applications, e.g., chance-constrained optimization.

Let β_1 represent the square of skewness and β_2 represent the kurtosis. We use the β_1–β_2 plane to illustrate the superiority of the Johnson system. The β_1–β_2 plane is shown in Fig. 1. Evidently, any probability distribution corresponds to a point on this plane.

In Fig. 1, β_1–$\beta_2 - 1 = 0$ denotes the boundary of skewness and kurtosis. The distribution does not exist beyond the boundary. The boundary curve of positive density of the Gram–Charlier series is the dotted line. The skewness and kurtosis of a distribution can only fall in the region enclosed by this boundary line and the coordinate axes [30], [36]; thus, the Gram–Charlier series can generate a PDF satisfying the probability theory. The S_L family forms a straight line on

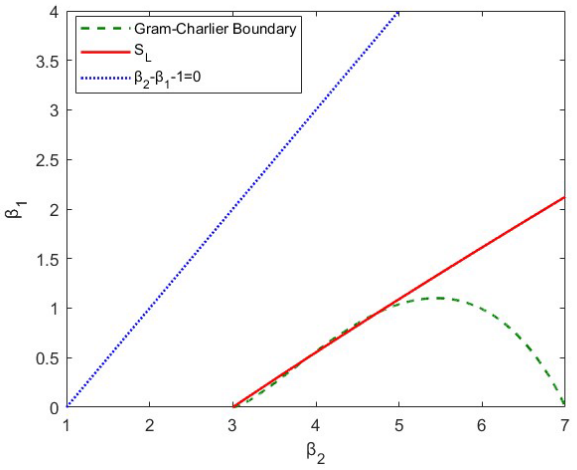

FIGURE 1. Feasible area of Johnson system and Gram–Charlier series on the β_1–β_2 plane.

the β_1–β_2 plane, dividing it into two areas. The upper and lower areas correspond to the S_B and S_U families, respectively. Evidently, the whole β_1–β_2 plane is covered by three families from the Johnson system, which is superior to the Gram–Charlier series and is a suitable choice to describe complicated distributions.

E. DETERMINING JOHNSON FAMILIES AND PARAMETERS

According to the previous analysis, approximating an arbitrary probability distribution can be accomplished by determining the proper families in the Johnson system and the corresponding parameters. Existing approaches include the quantile method [37] and the moment method [38], among others. The moment method requires information on the first four moments, which can be accurately estimated via BDR. Therefore, herein, using the moment method in conjunction with BDR is suitable to form a complete process. We now provide a simple description of the moment method.

The proper families are determined by calculating β_2' from

$$\beta_2' = \omega^4 + 2\omega^3 + 3\omega^2 - 3 \tag{20}$$

where ω is fixed by the skewness of the random variable:

$$\begin{aligned} \omega = &\frac{1}{2}(8 + 4\beta_1 + 4\sqrt{4\beta_1 + \beta_1^2})^{\frac{1}{3}} \\ &+ \frac{1}{2}(8 + 4\beta_1 + 4\sqrt{4\beta_1 + \beta_1^2})^{-\frac{1}{3}} - 1 \end{aligned} \tag{21}$$

If β_2' is close to β_2, the Lognormal distribution family S_L is selected. Otherwise, if $\beta_2' < \beta_2$, S_U is selected, and if $\beta_2\prime > \beta_2$, S_B is selected.

For S_L, the parameters have analytical expressions and can be calculated as follows:

$$\begin{aligned} a &= 0.5b \ln(\omega(\omega - 1)) \\ b &= \sqrt{\ln \omega} \\ c &= -\exp(\frac{0.5b - a}{b}) \\ d &= sign(\sqrt{\beta_1}) \end{aligned} \tag{22}$$

For S_U, the values of a and b are determined first; c and d are then calculated accordingly. If the random variable is a symmetric distribution ($\beta_1 \approx 0$), then, a and b are calculated as follows:

$$\begin{aligned} a &= 0 \\ b &= \sqrt{\ln \zeta} \\ \zeta &= \sqrt{\sqrt{(2\beta_2 - 2)} - 1} \end{aligned} \tag{23}$$

Otherwise, iterative calculations are necessary to determine a, b, and ζ.

After obtaining a and b, c and d are calculated as follows:

$$\begin{aligned} d &= (\frac{1}{2}(\zeta - 1)(\zeta \cosh(\frac{2a}{b}) + 1))^{-\frac{1}{2}} \\ c &= d\sqrt{\zeta} \sinh(\frac{a}{b}) \end{aligned} \tag{24}$$

For S_B, the parameters are iteratively calculated.

The detailed process of iteration for S_U and S_B can be found in Ref [38].

IV. PROCEDURE OF COMPUTATION

The proposed PLF method based on BDR and the Johnson system is presented step by step in this section, as follows:

1) Prepare the necessary data. The base data of the power system are required, along with samples of IRVs, which can be generated randomly or collected from historical data.

2) Obtain the correlation coefficient matrix of IRVs $\boldsymbol{\rho_X}$, and then calculate its corresponding coefficient matrix $\boldsymbol{\rho_Z}$ in standard Gaussian space.

3) Carry the Cholesky decomposition to $\boldsymbol{\rho_Z}$ and obtain the corresponding lower triangular matrix $\mathbf{L_Z}$.

4) Determine the abscissas and weights for the Gauss–Hermite quadrature scheme in the independent standard Gaussian space. Then, transform the abscissas to the points in original space according to (6).

5) Perform the DLF for the constant function and univariate functions of (12).

6) Judge whether the joint effect is minor based on (19) and ε. If it can be ignored, use (18) to calculate the bivariate function; if not, use (17).

7) Calculate the first four moments of the output variable from (13), (14), and (15).

8) Determine the proper families and parameters in the Johnson system according to the calculated moments.

9) Approximate the probability distribution of the ORVs.

V. CASE STUDIES

In this section, the proposed method is tested on a modified IEEE 118-bus system [39]. The DLF program is based on MATPOWER 6.0 [40] and is executed on a PC with a 2.8-GHz CPU and 16 GB RAM.

Assume that eight wind farms are integrated in the test system and are clustered into two groups. The total load of the system is 4243 MW, and the total wind power installed is 1320 MW; therefore, the penetration level of the wind power is about 30%, a significant degree of penetration. The wind farm locations, groups, and the rated power are listed in Table 2.

TABLE 2. Parameters of wind farms.

WF	Bus	Group	Rated power/MW
1–4	2,3,14,16	1	180
5–8	44,50,52,53	2	180

TABLE 3. Uncertainty description of wind farms.

Cases	WF	Distribution parameters	Fluctuation range/ MW	Max fluctuation power/ MW
Case I	1–4	Weibull (4.72, 1.64)	0-180	149.52
	5–8	Weibull (6.38, 3.43)	0-137.21	131.93
Case II	1–4	Beta (4.21, 1.82)	12.61-144	87.73
	5–8	Beta (0.83, 1.46),	0-144	91.29

To test the adaptability of the proposed method to IRV distribution, two cases using typical distribution that can represent the uncertainty of wind are performed.

In the first case, we assume the wind speed to be following Weibull distribution, which is a widely used distribution that represents the long-term uncertainty of wind speed. The wind power output is determined using the speed–power curve [5] as follows:

$$P = \begin{cases} 0 & \text{if } wv < wv_{in}^c \text{ or } wv < wv_{out}^c \\ \frac{wv - wv_{in}^c}{wv_{rated}^c - wv_{in}^c} P_{rated} & \text{if } wv_{in}^c < v < wv_{rated} \\ P_{rated} & \text{else} \end{cases} \tag{25}$$

where P_{rated} is the rated power of the wind turbine, P is the generated power of the turbine, wind turbines of the same wind farm are assumed to be integrated into one, v is the wind speed, wv_{in}^c and wv_{out}^c are cut-in and cut-out wind speed, respectively, and wv_{rated}^c is the rated wind speed of the wind turbine. In this case, we assume $wv_{in}^c = 2\ m/s$, $wv_{out}^c = 25m/s$, and $wv_{rated}^c = 13m/s$.

In the second case, wind power outputs are directly assumed to follow the Beta distribution, which is known to describe the short-term uncertainty of wind power properly [41]. The output of the windfarms is assumed to be 0.8 p.u. in this case.

The uncertainty description of wind farms in the two cases are summarized in Table 3.

In both cases, wind power outputs of the wind farm in the same group are assumed to be highly correlated, and there is no correlation between distinct groups. The correlation matrices of the wind power outputs are as follows:

$$\begin{aligned} \rho_{group1} &= \begin{bmatrix} 1 & 0.72 & 0.83 & 0.69 \\ 0.72 & 1 & 0.78 & 0.81 \\ 0.83 & 0.78 & 1 & 0.74 \\ 0.69 & 0.81 & 0.74 & 1 \end{bmatrix} \\ \rho_{group2} &= \begin{bmatrix} 1 & 0.81 & 0.63 & 0.67 \\ 0.81 & 1 & 0.73 & 0.85 \\ 0.63 & 0.73 & 1 & 0.79 \\ 0.67 & 0.85 & 0.79 & 1 \end{bmatrix} \end{aligned} \tag{26}$$

TABLE 4. Average relative error index.

Cases	Method	Type of ORV	$\bar{\varepsilon}_1$ (%)	$\bar{\varepsilon}_2$ (%)	$\bar{\varepsilon}_3$ (%)	$\bar{\varepsilon}_4$ (%)
Case I	BDR	P	0.3828	1.1142	8.0474	3.3937
		Q	0.2101	1.1353	9.8692	4.7359
		V	0.0018	0.5694	13.5739	5.2444
		θ	0.0638	1.4461	7.8866	2.9593
	UDR	P	0.3682	1.2202	69.3976	49.9307
		Q	0.4133	3.0005	47.7015	48.1359
		V	0.0018	3.9878	33.0720	48.4250
		θ	0.1334	2.0489	117.5901	58.6692
	CM	P	7.1265	1.4756	10.2753	4.5959
		Q	5.1776	12.7176	33.3752	12.7292
		V	2.3307	13.0893	46.9151	16.7411
		θ	2.3616	2.5058	17.1085	5.6843
Case II	BDR	P	0.2545	0.1403	16.9663	3.4209
		Q	0.7009	0.2598	16.3092	4.9108
		V	0.0016	0.2606	9.6646	3.3329
		θ	0.0284	0.0970	20.5566	3.6132
	UDR	P	1.0632	4.5992	68.6584	50.6180
		Q	2.3489	5.0020	65.6709	50.3282
		V	0.0048	3.6421	29.0823	51.5321
		θ	0.1139	7.1891	54.4536	61.2928
	CM	P	6.1487	2.1241	20.9689	5.2549
		Q	10.8240	7.7008	45.1968	9.6448
		V	2.4239	9.1976	42.4928	10.6715
		θ	0.6612	2.4162	61.8334	4.6877

In both cases, the power factor is set as 0.95. We also assume that the uncertainty of the load at each bus follows a Gaussian distribution, with expectations of active and reactive power injections equal to the base case data, and standard deviations equal to 5% of the expectations.

The goal of the PLF algorithm is to obtain accurate PDF and CDF curves efficiently, and the accuracy relies on two aspects: moment estimation results and curve approximation method.

The moment estimation accuracy of the proposed BDR is compared with those of the UDR proposed in ref. [25], CM proposed in ref. [8], and 50000 times MCSM. Note that here, the number of abscissas of BDR is chosen as 5, and, for consistency, that of the compared UDR is adjusted to be the same.

To show the performance of the Johnson system, PDF and CDF curves obtained by the BDR + Johnson system were compared with those of the BDR + Gram–Charlier series. To show the overall performance of the proposed method (BDR + Johnson system), PDF and CDF curves obtained by the proposed method were compared with CM + Gram-Charlier series and the empirical curves from MCSM.

The average relative error index [8] is adopted to indicate the accuracy of the moment of the ORVs estimated using each method. The average relative error index is defined as follows:

$$\bar{\varepsilon}_i = \frac{1}{N_1}\sum_{j}^{N_1}\left|\frac{\gamma_{i,j}^{EV} - \gamma_{i,j}^{MC}}{\gamma_{i,j}^{MC}}\right| \times 100\% \tag{27}$$

where i refers to the i^{th} central moment; N_1 refers to the number of a type of ORV; j is the corresponding series number;

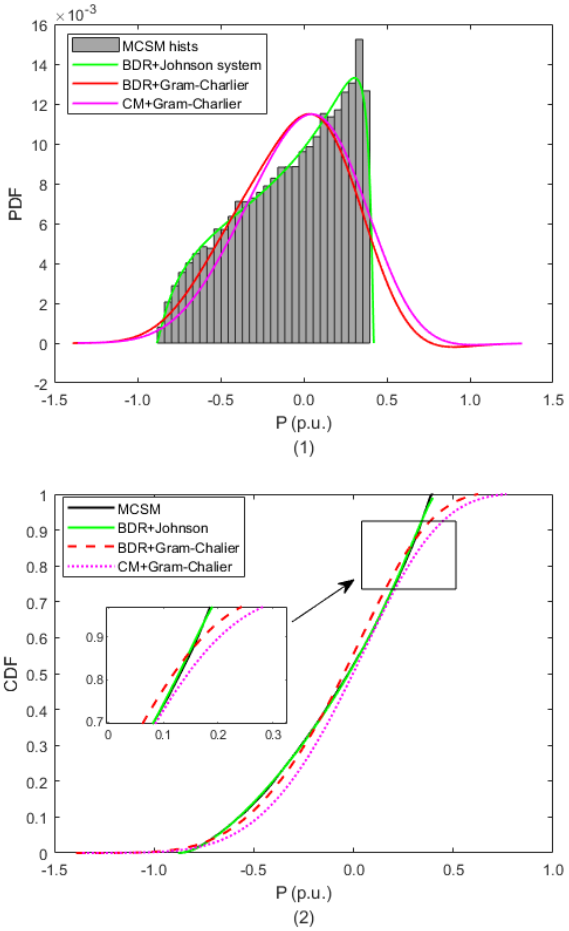

FIGURE 2. PDF (1) and CDF (2) of branch 49–50 active power flow.

and $\gamma_{i,j}^{MC}$ and $\gamma_{i,j}^{EV}$ refer to the results calculated by MCSM and the evaluated method, respectively.

The average relative error indices of the method being evaluated in this test system are listed in Table 4. Experience indicates that when using MCSM as a benchmark, a convergent skewness is difficult to obtain. Therefore, to obtain a relatively objective evaluation, if the absolute value of skewness of an ORV calculated by MCSM is less than 0.05, we do not include it in the statistics.

The data presented in Table 4 show that the BDR has the smallest estimation error for the first four moments in both cases. Comparing BDR and UDR, in estimating high-order moments, BDR significantly outperforms UDR in terms of precision. The maximum average relative error calculated by BDR is 3.6132% of kurtosis of θ, whereas the mean relative error of kurtosis of θ based on the UDR is as high as 61.2928% (too high for practical use). Evidently, considering the joint effects of the IRVs significantly reduces the estimation error of high-order moments. For CM, as the penetration level of these two cases is high and the wind power output is highly discrete, the linearization assumption is not valid, resulting in low accuracy.

The average relative error of the third moment (skewness) is high for all evaluated methods because of its small value

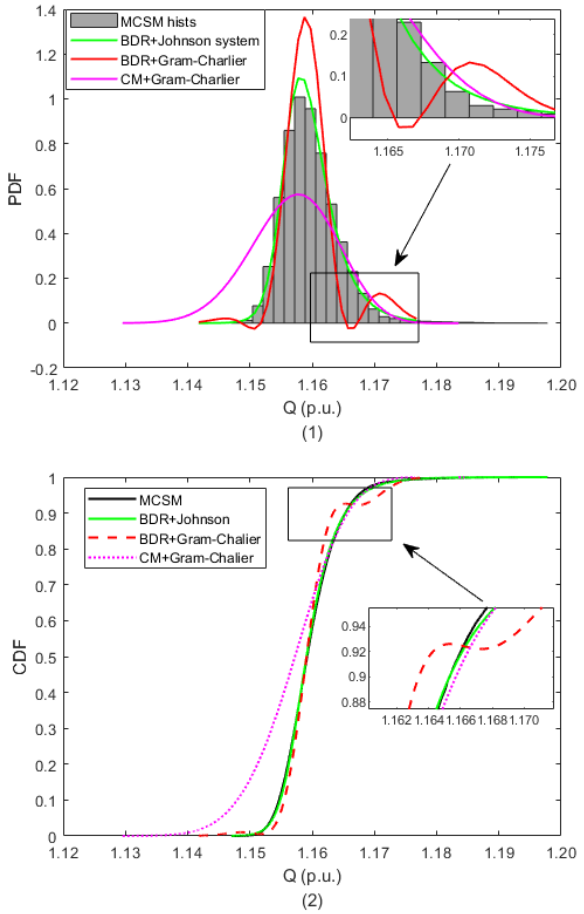

FIGURE 3. PDF (1) and CDF (2) of branch 5–8 reactive power flow.

and the instability of the benchmark as mentioned previously; however, its impact on approximating PDF and CDF curve, is relatively small.

We select the PDF and CDF of an active flow of branch 49–50 and reactive flow of branch 5–8 in case II as examples to show the effectiveness of the proposed method; the PDF and CDF curves are plotted in Figs. 2 and 3, respectively.

The PDF and CDF curve show that the BDR + Johnson system approximates well, whereas the BDR + Gram–Charlier series exhibits evident deviation, particularly in the tail area. In addition, the CDF approximated by the Gram–Charlier series in Fig. 3 exhibits a negative trend, violating the probability theorem. This renders the Gram–Charlier series unreliable in practical use. Evidently, for approximating the PDF and CDF of non-Gaussian variables, the Johnson system performs far better performance than Gram-Charlier series.

It can be found that the PDF and CDF curves obtained by the proposed method are very close to the MCSM results, so the overall accuracy of the proposed method is verified. There are two reasons that CM + Gram–Charlier series performs poorly in these two examples. One is the inaccuracy of moment estimation, and another is that the distribution of ORV has non-Gaussian characteristics and the point on the β_1–β_2 plane is out of the Gram-Charlier series boundary line.

TABLE 5. Comparison of the cdf approximation.

CDF	Method	ARMS (%)	CDF difference (p.u.) 1%	10%	90%	99%
$P_{49\text{-}50}$	BDR + Johnson system	0. 0018	0.0276	0.0004	0.0073	0.0172
	BDR + Gram–Charlier series	0. 0068	0.0936	0.0342	0.0197	0.1183
	CM + Gram–Charlier series	0.0120	0.7079	0.4893	0.4102	0.4678
$Q_{5\text{-}8}$	BDR + Johnson system	0.0071	0.0002	0.0002	7.4196e-06	8.6621e-05
	BDR + Gram–Charlier series	0.0407	0.0028	0.0008	0.0019	0.0009
	CM + Gram–Charlier series	0.1349	0.0208	0.0175	0.0282	0.0367

TABLE 6. Comparison of calculation speed.

	CM	PEM	BDR–JOHNSON	MCSM
Time (s)	1.25	7.83	43.63	390.91

As the CDF curve is more useful in applications based on PLF, such as Chance-constrained optimization, the average root mean square (ARMS) [28] is introduced to quantitatively indicate the accuracy of the CDF approximation:

$$ARMS = \frac{\sqrt{\sum_{i}^{N}(C_{MC,i} - C_i)^2}}{N_2} \times 100\% \tag{28}$$

where $C_{MC,i}^{\xi}$ and C_i^{ξ} refer to the i^{th} value on the CDF curves of the MCSM and evaluated methods, respectively; N_2 is the number of points at which the CDFs have been evaluated.

To demonstrate the performance of CDF approximation in the tail area, the absolute difference between the CDF values obtained via MCSM and the evaluated method at quantiles of 1%, 10%, 90%, and 99% are introduced.

Detailed data on CDF approximation performance are listed in Table 5. Evidently, the proposed method is superior with respect to all indices.

Table 6 shows the time consumed by the proposed method; although it is longer than that taken for the UDR and CM, it is significantly shorter than that taken for MCSM, showing that BDR has the potential to meet the timeliness requirements of online analysis.

VI. CONCLUSION

Currently and in the future, dealing with the uncertainties and complicated probability distributions involved in the utilization of RESs is a challenge for power system engineering. To ensure computational accuracy and efficiency in PLF calculations, a new PLF method based on BDR and the Johnson system is proposed in this study. The proposed method uses BDR to calculate the moments of the ORVs, thus avoiding the difficulties that PEM-based methods encounter in estimating high-order moments. Furthermore, the probability

distributions of the output variables are approximated by the Johnson system; in this manner, the defects of the series expansion-based method are eliminated. The proposed method can achieve a better performance in terms of accuracy or efficiency than PEM, CM, or MCSM when considering correlated, highly discrete, and non-Gaussian IRVs.

In the future, other computationally efficient methods such as principal component analysis or parallel computing can be studied and combined with the proposed method to further enhance efficiency. Nonlinear correlation theories, such as the copula theory may also combine with the proposed method to enhance accuracy and adaptability. The method may also prove useful for other PLF-based applications, such as probabilistic optimal load flow and chance-constrained optimization.

REFERENCES

[1] B. Borkowska, "Probabilistic load flow," *IEEE Trans. Power App. Syst.*, vol. PAS-93, no. 3, pp. 752–759, May 1974.
[2] B. R. Prusty and D. Jena, "A critical review on probabilistic load flow studies in uncertainty constrained power systems with photovoltaic generation and a new approach," *Renew. Sustain. Energy Rev.*, vol. 69, pp. 1286–1302, Mar. 2017.
[3] Y. Chen, J. Wen, and S. Cheng, "Probabilistic load flow method based on Nataf transformation and Latin hypercube sampling," *IEEE Trans. Sustain. Energy*, vol. 4, no. 2, pp. 294–301, Apr. 2013.
[4] D. Cai, D. Shi, and J. Chen, "Probabilistic load flow with correlated input random variables using uniform design sampling," *Int. J. Electr. Power Energy Syst.*, vol. 63, pp. 105–112, Dec. 2014.
[5] L. Zhang, H. Cheng, S. Zhang, P. Zeng, and L. Yao, "Probabilistic power flow calculation using the Johnson system and Sobol's quasi-random numbers," *IET Gener., Transmiss. Distrib.*, vol. 10, no. 12, pp. 3050–3059, Sep. 2016.
[6] L. Bin, M. Shahzad, Q. Bing, M. U. Shoukat, M. Shakeel, and E. K. Mohammedsaeed, "Probabilistic computational model for correlated wind farms using copula theory," *IEEE Access*, vol. 6, pp. 14179–14187, 2018.
[7] P. Zhang and S. T. Lee, "Probabilistic load flow computation using the method of combined cumulants and Gram–Charlier expansion," *IEEE Trans. Power Syst.*, vol. 19, no. 1, pp. 676–682, Feb. 2004.
[8] J. Usaola, "Probabilistic load flow with correlated wind power injections," *Electr. Power Syst. Res.*, vol. 80, no. 5, pp. 528–536, May 2010.
[9] Z. Hu and X. Wang, "A probabilistic load flow method considering branch outages," *IEEE Trans. Power Syst.*, vol. 21, no. 2, pp. 507–514, May 2006.
[10] A. Tamtum, A. Schellenberg, and W. D. Rosehart, "Enhancements to the cumulant method for probabilistic optimal power flow studies," *IEEE Trans. Power Syst.*, vol. 24, no. 4, pp. 1739–1746, Nov. 2009.
[11] Y. Yuan, J. Zhou, P. Ju, and J. Feuchtwang, "Probabilistic load flow computation of a power system containing wind farms using the method of combined cumulants and Gram–Charlier expansion," *IET Renew. Power Gener.*, vol. 5, no. 6, pp. 448–454, Nov. 2011.
[12] F. J. Ruiz-Rodriguez, J. C. Hernández, and F. Jurado, "Probabilistic load flow for photovoltaic distributed generation using the Cornish–Fisher expansion," *Electr. Power Syst. Res.*, vol. 89, pp. 129–138, Aug. 2012.
[13] B. R. Prusty and D. Jena, "Combined cumulant and Gaussian mixture approximation for correlated probabilistic load flow studies: A new approach," *CSEE J. Power Energy Syst.*, vol. 2, no. 2, pp. 71–78, Jun. 2016.
[14] M. Tourandaz Kenari, M. S. Sepasian, M. Setayesh Nazar, and H. A. Mohammadpour, "Combined cumulants and Laplace transform method for probabilistic load flow analysis," *IET Gener., Transmiss. Distrib.*, vol. 11, no. 14, pp. 3548–3556, Sep. 2017.
[15] T. Williams and C. Crawford, "Probabilistic load flow modeling comparing maximum entropy and Gram–Charlier probability density function reconstructions," *IEEE Trans. Power Syst.*, vol. 28, no. 1, pp. 272–280, Feb. 2013.
[16] W. Wu, X. Jiang, Z. Wang, G. Li, and K. Wang, "Probabilistic load flow calculation using cumulants and multiple integrals," *IET Gener., Transmiss. Distrib.*, vol. 10, no. 7, pp. 1703–1709, May 2016.
[17] C.-L. Su, "Probabilistic load-flow computation using point estimate method," *IEEE Trans. Power Syst.*, vol. 20, no. 4, pp. 1843–1851, Nov. 2005.
[18] H. P. Hong, "An efficient point estimate method for probabilistic analysis," *Rel. Eng. Syst. Saf.*, vol. 59, no. 3, pp. 261–267, Mar. 1998.
[19] J. M. Morales and J. Perez-Ruiz, "Point estimate schemes to solve the probabilistic power flow," *IEEE Trans. Power Syst.*, vol. 22, no. 4, pp. 1594–1601, Nov. 2007.
[20] C. S. Saunders, "Point estimate method addressing correlated wind power for probabilistic optimal power flow," *IEEE Trans. Power Syst.*, vol. 29, no. 3, pp. 1045–1054, May 2014.
[21] C. Chen, W. Wu, B. Zhang, and H. Sun, "Correlated probabilistic load flow using a point estimate method with Nataf transformation," *Int. J. Electr. Power Energy Syst.*, vol. 65, pp. 325–333, Feb. 2015.
[22] Y.-G. Zhao and T. Ono, "New point estimates for probability moments," *J. Eng. Mech.*, vol. 126, no. 4, pp. 433–436, Apr. 2000.
[23] B. Zou and Q. Xiao, "Probabilistic load flow computation using univariate dimension reduction method," *Int. Trans. Electr. Energy Syst.*, vol. 24, no. 12, pp. 1700–1714, Dec. 2014.
[24] Q. Xiao, S. Zhou, L. Wu, Y. Zhao, and Y. Zhou, "Investigating univariate dimension reduction model for probabilistic power flow computation," *Electr. Power Compon. Syst.*, vol. 47, nos. 6–7, pp. 561–572, Apr. 2019.
[25] Q. Xiao, Y. He, K. Chen, Y. Yang, and Y. Lu, "Point estimate method based on univariate dimension reduction model for probabilistic power flow computation," *IET Gener., Transmiss. Distrib.*, vol. 11, no. 14, pp. 3522–3531, Sep. 2017.
[26] X. Sun, Q. Tu, J. Chen, C. Zhang, and X. Duan, "Probabilistic load flow calculation based on sparse polynomial chaos expansion," *IET Gener., Transmiss. Distrib.*, vol. 12, no. 11, pp. 2735–2744, Jun. 2018.
[27] F. Ni, P. H. Nguyen, and J. F. G. Cobben, "Basis-adaptive sparse polynomial chaos expansion for probabilistic power flow," *IEEE Trans. Power Syst.*, vol. 32, no. 1, pp. 694–704, Jan. 2017.
[28] M. Fan, V. Vittal, G. T. Heydt, and R. Ayyanar, "Probabilistic power flow studies for transmission systems with photovoltaic generation using cumulants," *IEEE Trans. Power Syst.*, vol. 27, no. 4, pp. 2251–2261, Nov. 2012.
[29] Z. Wang, C. Shen, F. Liu, X. Wu, C.-C. Liu, and F. Gao, "Chance-constrained economic dispatch with non-Gaussian correlated wind power uncertainty," *IEEE Trans. Power Syst.*, vol. 32, no. 6, pp. 4880–4893, Nov. 2017.
[30] N. L. Johnson, "Systems of frequency curves generated by methods of translation," *Biometrika*, vol. 36, nos. 1–2, pp. 149–176, Jun. 1949.
[31] I. Usta and Y. M. Kantar, "Analysis of some flexible families of distributions for estimation of wind speed distributions," *Appl. Energy*, vol. 89, no. 1, pp. 355–367, Jan. 2012.
[32] H. Li, Z. Lü, and X. Yuan, "Nataf transformation based point estimate method," *Sci. Bull.*, vol. 53, no. 17, pp. 2586–2592, Sep. 2008.
[33] H. Xu and S. Rahman, "A generalized dimension-reduction method for multidimensional integration in stochastic mechanics," *Int. J. Numer. Methods Eng.*, vol. 61, no. 12, pp. 1992–2019, Nov. 2004.
[34] H. Rabitz, "General foundations of high-dimensional model representations," *J. Math. Chem.*, vol. 25, no. 2, pp. 197–233, 1999.
[35] W. Fan, J. Wei, A. H.-S. Ang, and Z. Li, "Adaptive estimation of statistical moments of the responses of random systems," *Probabilistic Eng. Mech.*, vol. 43, pp. 50–67, Jan. 2016.
[36] N. R. Draper and D. E. Tierney, "Regions of positive and unimodal series expansion of the Edgeworth and Gram–Charlier approximations," *Biometrika*, vol. 59, no. 2, pp. 463–465, 1972.
[37] R. E. Wheeler, "Quantile estimators of Johnson curve parameters," *Biometrika*, vol. 67, no. 3, pp. 725–728, Dec. 1980.
[38] I. D. Hill, R. Hill, and R. L. Holder, "Algorithm AS 99: Fitting Johnson curves by moments," *Appl. Statist.*, vol. 25, no. 2, pp. 180–189, 1976.
[39] University of Washington Electrical Engineering. *Power System Test Case Archive*. Accessed: Jan. 1, 2018. [Online]. Available: http://www.ee.washington.edu/research/pstca
[40] R. D. Zimmerman, C. E. Murillo-Sanchez, and R. J. Thomas, "MATPOWER: Steady-state operations, planning, and analysis tools for power systems research and education," *IEEE Trans. Power Syst.*, vol. 26, no. 1, pp. 12–19, Feb. 2011.
[41] H. Bludszuweit, J. A. Dominguez-Navarro, and A. Llombart, "Statistical analysis of wind power forecast error," *IEEE Trans. Power Syst.*, vol. 23, no. 3, pp. 983–991, Aug. 2008.

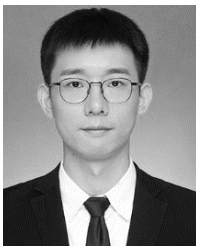

HANG LI was born in 1991. He received the B.Eng. degree from the Huazhong University of Science and Technology (HUST), in 2013, where he is currently pursuing the Ph.D. degree. His research interests include power system analysis and operation with renewable energy integration.

ZHE ZHANG received the Ph.D. degree in electrical engineering from the Huazhong University of Science and Technology (HUST), Wuhan, China, in 1992. He is currently a Professor with the College of Electrical and Electronic Engineering, HUST. His research interests include power system analysis and protective relaying.

XIANGGEN YIN (Member, IEEE) received the B.S., M.S., and Ph.D. degrees in electrical engineering from the Huazhong University of Science and Technology (HUST), Wuhan, China, in 1982, 1985, and 1989, respectively. He is currently a Professor with the School of Electrical and Electronic Engineering, HUST. His research interests include power system analysis, fault location, protective relaying, and power system stability control.